

Supplementary Information

Nanoplasmonics tuned “click chemistry”

Inga Tijunelyte¹, Erwann Guenin¹, Nathalie Lidgi-Guigui¹, Florent Colas², Joyce Ibrahim³, Timothée Toury³, Marc Lamy de la Chapelle¹

¹*Université Paris13, Sorbonne Paris Cité, Laboratoire CSPBAT, CNRS, (UMR7244), 74 rue Marcel Cachin, 93017 Bobigny, France*

²*IFREMER, Centre de Brest, Interfaces and Sensors and Group, BP 70, 29280 Plouzané, France*

³*Université de Technologie de Troyes, Laboratoire de Nanotechnologie et d'Instrumentation Optique, Institut Charles Delaunay, FRE 2848, 12 rue Marie Curie, 10004 Troyes, France*

Keywords: Thiol-ene click chemistry, SERS, nanoplasmonics

Corresponding author: marc.lamydelachapelle@univ-paris13.fr

1. Investigation on thiol-ene reaction initiation conditions

In the article described results demonstrate successful thiol-ene reaction initiation thanks to physical effects provided by highly resonant NCs. For this reaction 2,2'-Azobis(2-methylpropionamide) dihydrochloride (AAPH) was used as a radical initiator.

In order to test this radical initiator performance in bulk conditions we have performed the thiol-ene reaction under several experimental conditions. The aqueous reaction mixture was first prepared by dissolving one equivalent of both: thiophenol (3.5 μL , 7 mmol.L^{-1}) and pentenoic acid (3.5 μg , 7 mmol.L^{-1}). This acid has been used to mimic the allyl mercaptan since the latter one has a thiol group that could directly react with the double bond of another allyl mercaptan molecule. In such conditions, it will not be able to determine the actual efficiency of the thiol-ene reaction between the thiophenol and the mercaptan. Thus we have used the pentenoic acid that have no thiol group but still have a double bond for thiol-ene reaction. Since this acid and the allyl mercaptan have similar structure, we assume that the reaction rate is also similar for both molecules. The mixture was investigated by Nuclear Magnetic Resonance (NMR) in deuterium oxide (D_2O) using Bruker Avance III 400 MHz instrument prior to the initiation of thiol-ene reaction. The figure S1 shows the ^1H NMR spectrum of the region of interest. Multiple peaks presented in ^1H NMR spectrum at 4.81-5.07 (m, 2H) and 5.78-5.9 (m, H) are assigned to the vinyl protons whereas the group of peaks at 7.11-7.34 (m, 5H) belongs to the aromatic protons.

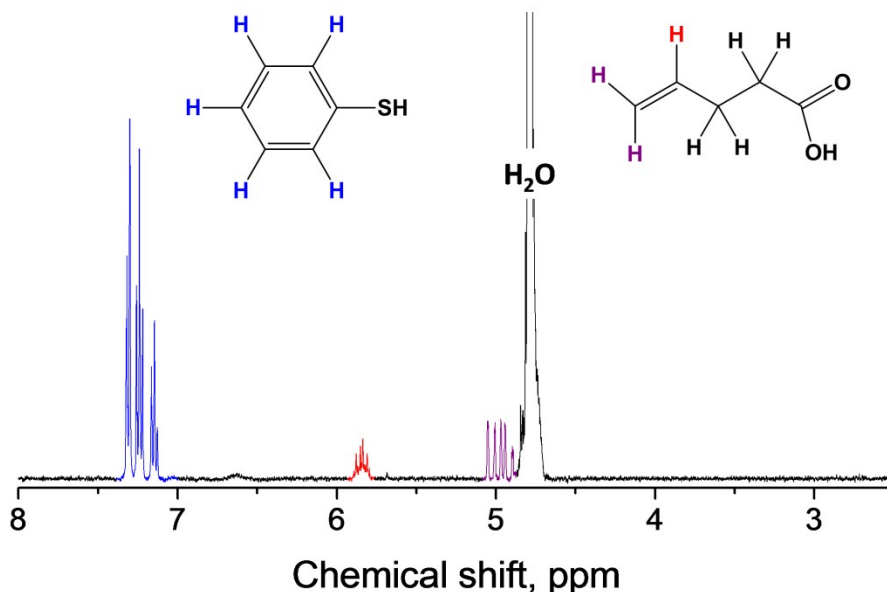


Figure S1 Nuclear Magnetic Resonance (NMR) spectrum of thiophenol and pentenoic acid mixture

After introducing the AAPH (9.5 mg, 7 mmol.L⁻¹) in solution, four different initiation conditions were performed (Figure S2.):

- 1) illumination of the solution with 660 nm laser light with a power of 0.45 mW (these conditions correspond to the exact ones used with the NCs)
- 2) illumination of the solution with 660 nm laser light with a power of 4.5 mW
- 3) heating of the solution at 60 °C
- 4) illumination of the solution with UV excitation wavelength of 365 nm

For all experiments, the exposure time (illumination or heating) was set to 30 min. The thiol-ene reaction in bulk was monitored by ¹H NMR thanks to the observation of multiple peaks at 7.48 ppm and 2.71 ppm (a and b labels on the figure S2, respectively). The first peaks correspond to a shift of protons from the aromatic ring whereas the peaks at 2.71 ppm are assigned to the protons of the carbon bound to sulfur¹. No spectral changes were observed on the NMR spectra after irradiating the mixture using identical parameters as the ones described in article (laser of 660 nm with the power of 0.45 mW) and even after increasing the laser power by one order of magnitude (power of 4.5 mW). The reaction starts at very low level after incubating solution at 60°C (observation of peaks with very low intensity at 2.71 and 7.48 ppm). This observation is not surprising. In the literature, the use of AAPH for radical reaction demands heating to 60°C for 24h². The highest reaction efficiency was observed by irradiating sample under UV light since after 30 minutes of illumination intense bands are observable.

These results indicate clearly that the thiol-ene reaction cannot be initiated using the 660 nm excitation wavelength even if the laser power density is high without any plasmonic structures. Moreover, the reaction is slow using the increase of the temperature or the UV light. It means that the plasmonic effect enhance the chemical process and accelerate the thiol-ene reaction at the nanostructure surface.

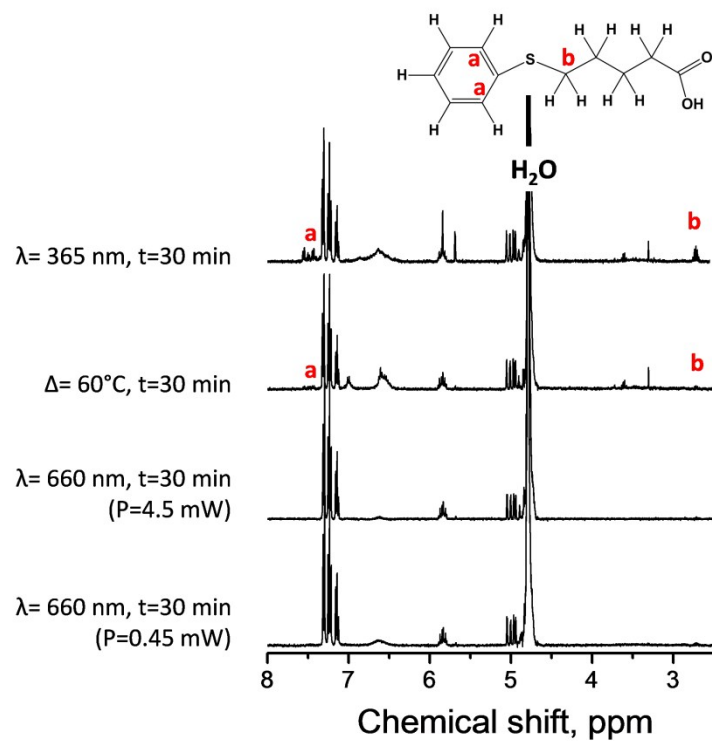


Figure S2 Nuclear Magnetic Resonance (NMR) spectra recorder after exposing mixture for thiol-ene reaction to a various initiation conditions.

2. SERS spectra recorded for the different experiments

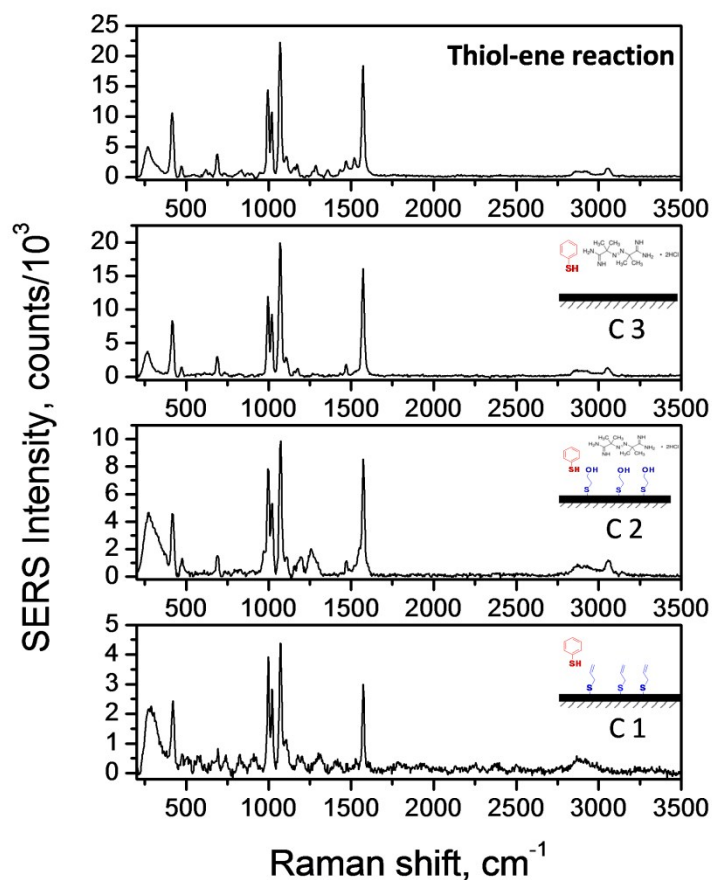


Figure S3 SERS spectra of thiophenol grafted to gold NCs *via* competitive replacement (experiments C1 and C2), spontaneous adsorption (experiment C3) or thiol-ene chemistry.

The comparison of the SERS spectra obtained after thiophenol grafting by thiol-ene reaction or by spontaneous or competitive interactions is presented on Figure S3. Except the first negative control (C1) all other SERS substrates were initially pre-functionalized by either allyl mercaptan or mercaptoethanol. After the thiophenol immobilization, all SERS spectra exhibit very similar spectral features that can be assigned to the main fingerprints of thiophenol. This means that the grafting of the thiophenol did not change its structure or its orientation on the gold surface. Moreover, the contribution of the allyl mercaptan or mercaptoethanol is actually limited to the SERS spectra which are dominated by the thiophenol contribution.

3. Temperature calculation

When light is absorbed by a nanoparticle (NP), part of the incoming energy is turned into heat, leading to an increase of the NP temperature (ΔT_0) and as a consequence inducing a local heat of the surrounding media. ΔT_0 is directly related to the absorption cross-section (σ_{abs}) as³:

$$\Delta T_0 = \frac{\sigma_{abs} I_{inc}}{4\pi R_{eff} \beta \kappa_{surr}} \quad \text{Eq. 1}$$

with I_{inc} the irradiance of the incoming beam in the plane of the NP, R_{eff} the effective radius of the NP (defined as the radius of a sphere of a volume equals to that of the NP), β a constant depending on the aspect ratio of the NC and κ_{surr} the thermal capacity of the surrounding medium. In our case, κ_{surr} is considered as the mean of the thermal capacity of water and glass ($\kappa_{surr} \approx 1 \text{ Wm}^{-1} \text{ K}^{-1}$).

In the case of an assembly of NPs, the heating transfer from one NP to the others contributes to the temperature increase. Considering a Gaussian beam of waist (w_0) shining an array of NPs, the collective temperature increase is proportional to the absorption cross-section of the individual NP and a geometrical parameter as⁴:

$$\Delta T_{coll} = \frac{\sigma_{abs} I_{inc}}{\kappa_{surr}} \sqrt{\frac{\ln 2}{4\pi w_0 A}} \left(1 - \frac{4\sqrt{A \ln 2}}{\pi w_0} \right) \quad \text{Eq. 2}$$

where A is the area of the lattice. In the case of a square lattice of side length D , $A=D^2$.

The absorption cross-sections of the NC assembly in a square lattice arrangement were calculated by Discrete Dipole Approximation (DDA) using DDSCAT 7.3⁵. Their diameters varied from 100 to 200 nm while their height was kept constant to 50 nm. The interparticle distance was 200 nm. A chromium adhesion layer of 2 nm thickness was added underneath each NC. The relative permittivity of gold was taken from⁶ and that of the chromium from Sopra database. The interdipole distance was set to 2 nm as a balance between mesh resolution and memory requirements. The calculations were performed with the HPC facilities of Pôle de Calcul Intensif pour la Mer⁷.

The surrounding medium was modeled by an effective medium with relative permittivity ϵ_{eff} ⁸⁻¹⁰ equal to the mean of that of the glass substrate and that of water (Eq. 1).

$$\epsilon_{eff} = \epsilon_{glass} + \epsilon_{water} \quad \text{Eq. 1}$$

The absorption cross-sections calculated by DDA are shown on figure S4. The position of the

absorption band is red-shifted as the diameter of the NC increases. Unless for the two smallest diameters the value of the maximum is almost constant over the range of diameter considered. The best match between the laser wavelength of 660 nm and the resonance of NCs is reached for diameters of about 120-130 nm.

The temperature increases ($\Delta T = \Delta T_0 + \Delta T_{\text{coll}}$) were calculated from equations 1 and 2 for the different diameters when the NCs are illuminated by a Gaussian beam at a wavelength of 660 nm with a waist equal to the diffraction limit of the beam (1 μm) and with a power of 0.45 mW. The illumination conditions reproduce the experimental ones in order to determine the exact temperature reached above the NCs during the different chemical reaction (thiol-ene reaction and experiments from C1 to C3). The ΔT are plotted on figure S5. For small diameter NCs, the temperature increase rises with the diameter to reach 60 K with 120 nm NCs. ΔT then decreases with the diameter as the mismatch between the resonance and laser line gets larger.

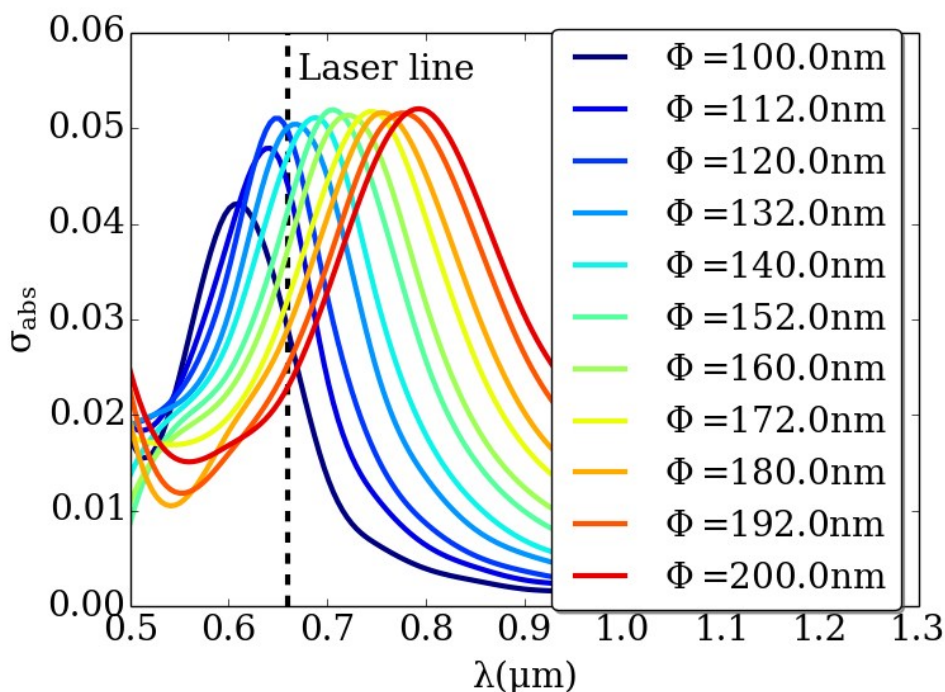


Figure S4: Absorption cross section calculated by DDA for the NC with diameter from 100 up to 200 nm. The dotted vertical line corresponds to the laser wavelength.

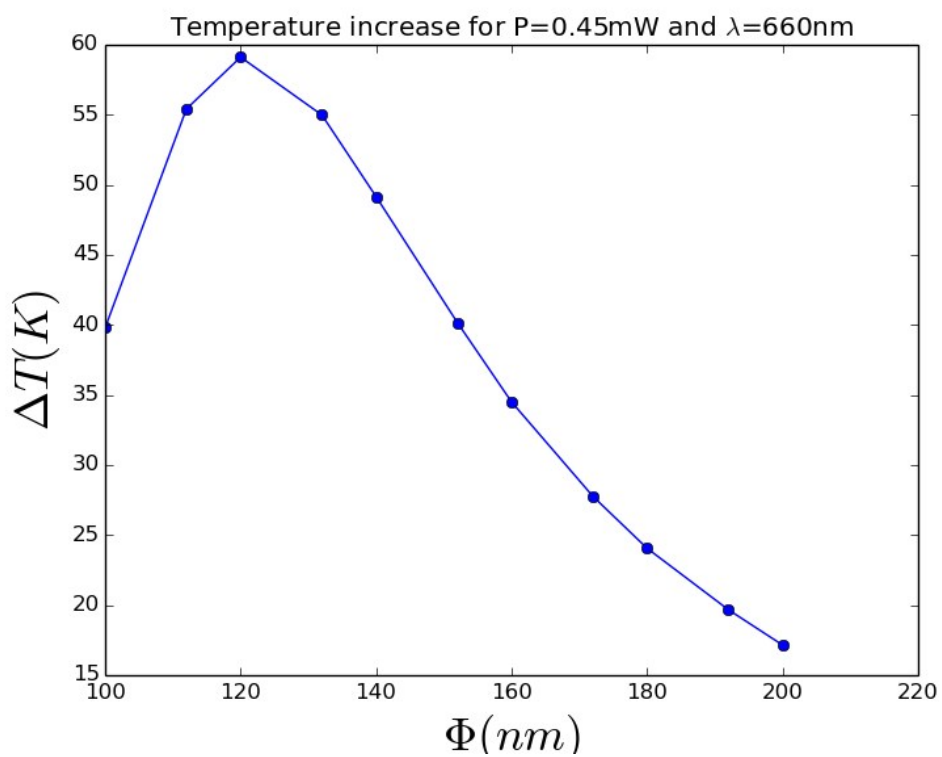


Figure S5: Temperature increase calculated around the NCs versus the NC diameter for an excitation wavelength of 660 nm and a power of 0.45 mW.

References:

1. P. Derboven, D. R. D'hooge, M. M. Stamenovic, P. Espeel, G. B. Marin, F. E. Du Prez and M.-F. Reyniers, *Macromolecules*, 2013, **46**, 1732-1742.
2. D. Dupin, A. Schmid, J. A. Balmer and S. P. Armes, *Langmuir*, 2007, **23**, 11812-11818.
3. G. Baffou, R. Quidant and F. J. García de Abajo, *ACS Nano*, 2010, **4**, 709-716.
4. G. Baffou, P. Berto, E. Bermúdez Ureña, R. Quidant, S. Monneret, J. Polleux and H. Rigneault, *ACS Nano*, 2013, **7**, 6478-6488.
5. B. T. Draine and P. J. Flatau, *Journal of the Optical Society of America A*, 1994, **11**, 1491-1499.
6. P. B. Johnson and R. W. Christy, *Physical Review B*, 1972, **6**, 4370-4379.
7. <http://www.ifremer.fr/pcim>).
8. M. Pelton, J. Aizpurua and G. Bryant, *Laser & Photonics Reviews*, 2008, **2**, 136-159.
9. D. Barchiesi, S. Kessentini, N. Guillot, M. L. de la Chapelle and T. Grosjes, *Opt Express*, 2013, **21**, 2245-2262.
10. D. Barchiesi, *Opt Express*, 2012, **20**, 9064-9078.